A Coloring Book Approach
to Finding Coordination Sequences

C. Goodman-Strauss
SCEN 303
Univ. Arkansas
Fayetteville, AR 72701, USA
strauss@uark.edu

N. J. A. Sloane
The OEIS Foundation Inc.
11 South Adelaide Ave.
Highland Park, NJ 08904, USA
njasloane@gmail.com

April 2, 2018

To our friend John H. Conway.

Abstract An elementary method is described for finding the coordination sequences for a tiling, based on coloring the underlying graph. We illustrate the method by first applying it to the two kinds of vertices (tetravalent and trivalent) in the Cairo (or dual-$3^2.4.3.4$) tiling. The coordination sequence for a tetravalent vertex turns out, surprisingly, to be $1, 4, 8, 12, 16, \ldots$, the same as for a vertex in the familiar square (or 4^4) tiling. We thought that such a simple fact should have a simple proof, and this article is the result. We also apply the method to obtain coordination sequences for the $3^2.4.3.4$, $3.4.6.4$, 4.8^2, 3.12^2, and $3^4.6$ uniform tilings, as well as the snub-632 and bew tilings. In several cases the results provide proofs for previously conjectured formulas.

1 Introduction

The "Cairo tiling" (Figure 1) has many names, as we will see in Section 2. In particular, it is the dual of the snub version of the familiar square tiling. It has two kinds of vertices (i.e. orbits of vertices under its symmetry group) — tetravalent and trivalent.

It therefore has two coordination sequences (CS's), giving the numbers $a(n)$ of vertices that are at each distance n from a base vertex P, as measured in the graph of edges and vertices in the tiling: those based at either a trivalent or tetravalent vertex. These coordination sequences may be read off from the contour lines, of equal distance from the base vertex P (Figure 2, left and right, respectively). However, although contour lines are structured and can be used to compute CS's, they seem unwieldy to construct and work with.

This article was motivated by our recent discovery that the coordination sequence for a tetravalent vertex in the Cairo tiling appeared to be the same as that for the square grid. We thought that such a simple fact should have a simple proof, and this article is the result.

The *coloring book approach*, described in §3, is an elementary means of calculating coordination sequences, based on coloring the underlying graph with "trunks and branches" and finding a recurrence for the number of vertices at a given distance from the base point. We have to verify that a desired local structure propagates, and that our colored trees do give the correct distance to the base vertex. In §4 we illustrate the method by applying it to an elementary case, the 4^4 square grid tiling.

The method works quite well in many cases and is at least helpful in others: in Sections §5 and §6 we deal with the tetravalent and trivalent vertices in the Cairo tiling and in §7 with its dual, the uniform (or Archimedean) $3^2.4.3.4$ tiling. We then apply the method to obtain coordination sequences for four other uniform tilings, 3.4.6.4 (§8), 4.8^2 (§10), 3.12^2 (§11), $3^4.6$ (§12), to the dual of the $3^4.6$ (§13) tiling, and to an example of a different type, the *bew* net (§9).

Starting in §11 we must rely on a more subtle analysis, but find that the coloring book method at least renders our calculations somewhat more transparent. (Having the contour lines worked out certainly boosted our confidence in the details!)

There are of course many papers that discuss more sophisticated methods for calculating coordination sequences, in both the crystallographic and mathematical literature, such as [1, 2, 3, 9, 11, 12, 13, 14, 15, 16, 17, 23, 29, 30]. For a uniform tiling, where the symmetry group acts transitively on the vertices, there is an alternative method for finding CS's based on Cayley diagrams and the Knuth-Bendix algorithm, and using the computer algebra system Magma [6]. This is briefly described in §14.

A more traditional way to calculate the CS by hand is to draw 'contour lines' or 'level curves' that connect the points at the same distance from P. These lines are usually overlaid on top of the tiling. The resulting picture can get very complicated (see Fig. 2), and this approach is usually only successful for simple tilings or for finding just the first few terms of the CS.

"Regular production systems" [21] can be used to give a formal model of growth along a front, enabling generalized contour lines to be described as languages, and underlies some of our thinking here.

The computer program *ToposPro* [5] makes it easy to compute the initial terms of the coordination sequences for a large number of tilings, nets (both two- and three-dimensional), crystal structures, etc.

Besides the obvious application of coordination sequences for estimating the density of points in a tiling, another use is for identifying which tiling or net is being studied. This is especially useful when dealing with three-dimensional structures, cf. [23]. Another application of our coloring-book approach is for finding labels for the vertices in a graph, as we mention at the end of §3.

For any undefined terms about tilings, see the classic work [25], or the article [24].

2 The Cairo tiling

The Cairo tiling is shown in Fig. 1. This beautiful tiling has many names. It has been called the Cairo pentagonal tiling [37], the MacMahon net [30], the mcm net [34], the dual of the $3^2\dot{4}.3.4$ tiling [25, pp. 63, 96, 480 (Fig. P_5-24)], the dual snub quadrille tiling, or the dual snub square tiling [8, pp. 263, 288].
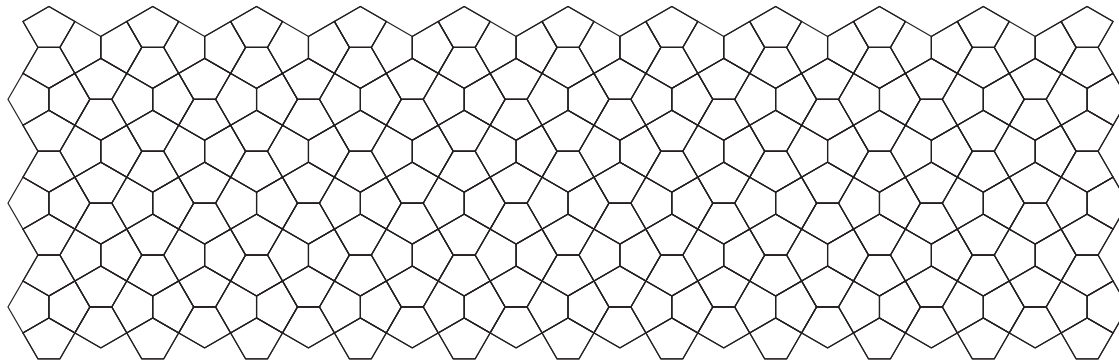

Figure 1: A portion of the Cairo tiling.

From the orbifold perspective of [8, Ch. 15], any periodic tiling is specified by a graph on an orbifold, and isohedral tilings have particularly simple ones, as for the Cairo tiling, in the figure below left. It is the dual of, in the doily notation for Archimedean tilings, $\langle 0 \rangle (12) * (3, 4, 3, 4, 3)$ [8, pp. 261], describing a quotient of collared edges on an orbifold (figure below, right):

We will refer to it simply as the Cairo tiling. There is only one shape of tile, an irregular pentagon, which may be varied somewhat. (We may change the tiling's geometry without affecting its combinatorics and coordination sequences, so long as we preserve the topology of the orbifold graph.)

Remarkably few decorative uses of this tiling are known, as David Bailey has extensively researched [4], and we have no example older than the floor of the Electoral Palace in Heidelberg, Germany, dating only to around 1900 [36]. The tiling is named from its use in Cairo, where this pentagonal tile has been mass-produced since at least the 1950's and is prominent around the city.

The CS with respect to a tetravalent vertex in the Cairo tiling begins

$$1, 4, 8, 12, 16, 20, 24, 28, 32, \ldots, \tag{1}$$

which suggests that it is the same as the CS of the familiar 4^4 square grid (sequence [A008574](#)[1] in [32]) . We will show in §5 that this is true, by proving:

---

[1]Six-digit numbers prefixed by A refer to entries in [32].

Theorem 1. *The coordination sequence with respect to a tetravalent vertex in the Cairo tiling is given by $a(0) = 1$, $a(n) = 4n$ for $n \geq 1$.*

The CS with respect to a trivalent vertex begins

$$1, 3, 8, 12, 15, 20, 25, 28, 31, 36, 41, 44, 47, 52, 57, 60, 63, 68, 73, 76, \dots, \tag{2}$$

which has now been added to [32] as sequence A296368. In §6 we will prove:

Theorem 2. *The coordination sequence with respect to a trivalent vertex in the Cairo tiling is given by $a(0) = 1, a(1) = 3, a(2) = 8$, and, for $n \geq 3$,*

$$
\begin{aligned}
a(n) &= 4n && \text{if } n \text{ is odd}, \\
&= 4n - 1 && \text{if } n \equiv 0 \pmod{4}, \\
&= 4n + 1 && \text{if } n \equiv 2 \pmod{4}.
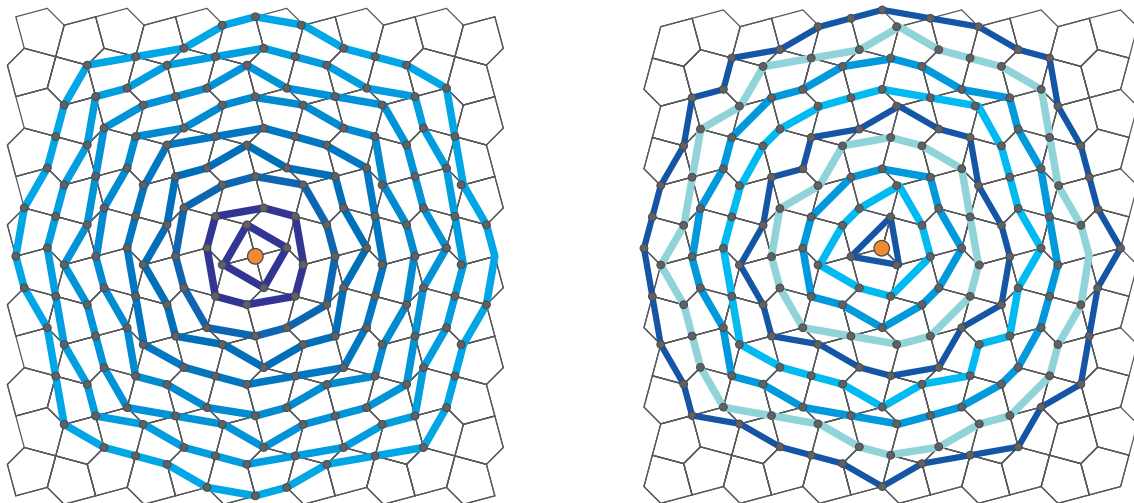\end{aligned} \tag{3}
$$

Figure 2: The Cairo tiling has two kinds of vertices (i.e., orbits of vertices under the $4*2$ symmetry group of the tiling) — tetravalent and trivalent. At left, the contour lines of constant distance from a central tetravalent vertex, from which we can read off the first several terms of its CS. At right, contours centered at a trivalent vertex (§6). These contour lines have a recursive and analyzable structure, but we find that the *coloring book* approach, shown in Figures 5 and 6, is much simpler, allowing more easily verifiable calculations.

The dual of the Cairo tiling is the uniform (or Archimedean) tiling $3^2.4.3.4$ shown in Fig. 3. Now there is only one kind of vertex, with valency 5, and the coordination sequence begins

$$1, 5, 11, 16, 21, 27, 32, 37, 43, 48, 53, 59, 64, 69, 75, 80, 85, 91, 96, 101, \dots, \tag{4}$$

given in A219529. That entry has a long-standing conjecture that $a(n) = \lfloor \frac{16n+1}{3} \rfloor$, and we will establish this in §7 by proving:

4

Theorem 3. *The coordination sequence with respect to a vertex in the $3^2.4.3.4$ tiling is given by* $a(0) = 1$,

$$
\begin{aligned}
a(3k) &= 16k, \ k \geq 1, \\
a(3k+1) &= 16k + 5, \ k \geq 0, \\
a(3k+2) &= 16k + 11, \ k \geq 0.
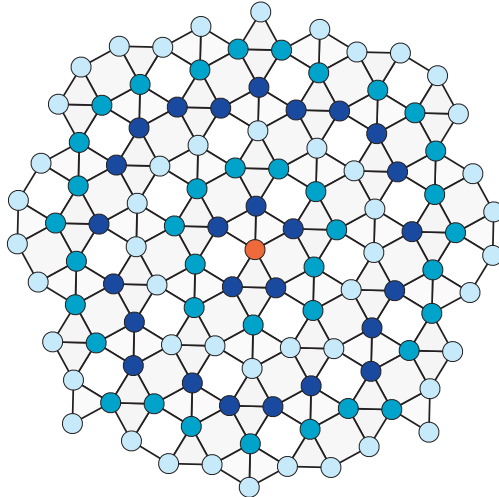\end{aligned}
\tag{5}
$$

Figure 3: A portion of the $3^2.4.3.4$ uniform tiling, the dual to the Cairo structure. Distances to P (which is the red vertex in the center of the figure) are shown in various colors, illustrating terms $a(0), \ldots, a(6)$ of the coordination sequence, A219529. In Figure 7, the count is clarified by a trunks and branches structure.

3 The coloring book approach to finding coordination sequences

We start with a more precise statement of the problem. Let T be a periodic tiling of the plane by polygonal tiles. The graph $G = G(T)$ of the tiling has a vertex for each point of the plane where three or more tiles meet, and an edge between two vertices if two tiles share a boundary along the line joining the corresponding points.

We assume the tiling is such that G is a connected graph: G is thus a connected, periodic, planar graph with all vertices of valency at least 3, and (since the tiles are polygons) with no parallel edges. The coloring book method could be applied to any such graph, not just those arising from tilings.

The distance $d(Q, R)$ between vertices Q, R in G is defined to be the number of edges in the shortest path joining them. The coordination sequence of G with respect to a vertex $P \in G$ is the sequence $\{a(n) : n = 0, 1, 2, \ldots\}$ where $a(n)$ is the number of vertices $Q \in G$ with $d(Q, P) = n$. We refer to P as the *base vertex*. For a periodic tiling there are only a finite number of different choices for the base vertex, and our goal is to find the coordination sequence with respect to a base vertex of each possible type.

Our method for finding the coordination sequence with respect to a base vertex P is to try to find a subgraph H of G with the following properties.

(i) H is a connected graph that passes through every vertex of G, and

(ii) for any vertex Q, every path in H from Q to P has the minimal possible length, $d(Q, P)$.

We also want H to have three further, less well-defined, properties.

(iii) H should be essentially a tree (in the sense of graph theory), and more precisely should consist of a finite number of "trunks" (in the arboreal sense), which are disjoint paths that originate at P, together with infinitely many "branches", which are also disjoint paths and originate at trunk vertices. However, on occasion we will allow the trunks to have "burls" (i.e., bulges, or loops inside the trunk), and both trunks and branches may have "twigs" (typically small subtrees with just a few edges) growing from them.

In our figures, trunks will usually be colored blue) and branches green. A glance at some of the figures below will illustrate our arboreal terminology. In Figs. 4, 5 (left), and 8 (left), H actually *is* a tree, with simple trunks and branches. In Fig. 6 (left) H is still a tree, but there are twigs (single edges) between the two parallel trunks. In Figs. 7 (left and right) two of the trunks have burls (loops of lengths 4 and 6, respectively), and so are not pure trees in the mathematical sense. In Fig. 12 both the trunks and branches have twigs attached.

(iv) There should an easy way to check that Property (ii) holds, i.e., that there are no shortcuts to P that take a path that is not part of H.

(v) And towards this end, H should some sort of regular structure that allows us to make inductive arguments.

There is no difficulty in satisfying (i), since any spanning tree rooted at P would do. But this is not very helpful since there are an infinite number of distinct spanning trees, and in any case requiring H to be a tree in the mathematical sense can make it harder to satisfy the other conditions.

Assuming that (ii) and (iii) hold, the subgraph H has the following structure. Each trunk out of P is an infinite path, and each trunk vertex (ignoring the slight complication caused by the burls) is joined to a unique trunk vertex that is one step further away from P. The branches are infinite paths originating at trunk vertices and (ignoring the twigs) each branch vertex is joined to a unique branch vertex that is one step further away from P. The twigs are finite (and small) subtrees that connect any remaining vertices to the closest trunk or branch. If we have carried out (v) well at all, then all these vertices should be easy to count.

An alternative way to describe H is to think of G as a topographic map, where the heights above sea level of the vertices are the distances from the base point P. Then H represents a drainage network that always flows downhill. In this model the 'trunks' represent major rivers that flow to P, and the 'branches' are tributaries that feed into the major rivers.

Speaking informally, the subgraph H is usually orthogonal to the contour lines, just as in polar coordinates, radial lines are orthogonal to the circles.

We have tried a few strategies for finding the subgraph H. In several examples (§7-§10), our human visual system seems to fill in the proof of Property (ii) instantly. But a verifiable means of testing (ii) is essential. For the Cairo tiling, we can redraw the graph so that (ii) is clear, as at right in Figures 5 and 6.

As described further in §12, in later examples we use an atlas of patterns, of what locally appear to be trunks and branches, directed across alleged contour lines. These patterns propagate outwards from a region about P — each patch extends outwards in a natural way. Since the alleged contour lines are initially simple nested closed curves, they continue to be so, and therefore are indeed contour lines. Since the alleged trunks and branches are transverse to the contour lines, they are indeed trunks and branches satisfying (ii).

We have found the process of searching for trunks and branches by drawing with colored pencils on pictures of tilings to be quite enjoyable. If readers wish to try this for themselves — and perhaps to improve on our constructions — we encourage them to download pictures of tilings from the Internet. There are many excellent web sites. Galebach's web site [20] is especially important, as it includes pictures of all k-uniform tilings with $k \leq 6$, with over 1000 tilings. The Chavey article [7] and the Hartley [26] and Printable Paper [33] web sites have many further pictures, and the RCSR [34] and ToposPro [5] databases have thousands more (see also [38]). We have collected a few of our favorites into [22]. There are potentially a very large number of coordination sequences of these tilings that could be added to the OEIS, with or without recurrences obtained by the coloring book method.

One's first guess at a trunks and branches structure does not always succeed. For example, in the 3.4.6.4 tiling, shown at right in Fig. 7, a natural first guess is to make the branches roughly horizontal. However, this does not provide the shortest paths to the origin — for that one needs to use vertical branches that head North-East (in the first quadrant) and North-West (in the second quadrant), as shown in the figure.

There is sometimes another side-benefit to our approach: it may provide a way to coordinatize the vertices of the graph. If the branches are paths, and a vertex Q is on a branch that originates at a trunk vertex R, then we can label Q by specifying the trunk, the distance $d(R, P)$, the branch, and the distance $d(Q, R)$ (with appropriate modifications in case the trunk or branch is not quite a simple path).

4   The square grid

Before analyzing the Cairo tiling, we illustrate the coloring book method by applying it to a simple case, the 4^4 square tiling seen in graph paper. The subgraph H is shown in Fig. 4.

For this tiling it is not hard to work out the CS directly, by drawing the contour lines, which are concentric squares centered at the origin. Each new square plainly contains four more vertices

than the last one, so the tiling's CS satisfies the recurrence $a(n+1) = a(n) + 4$.
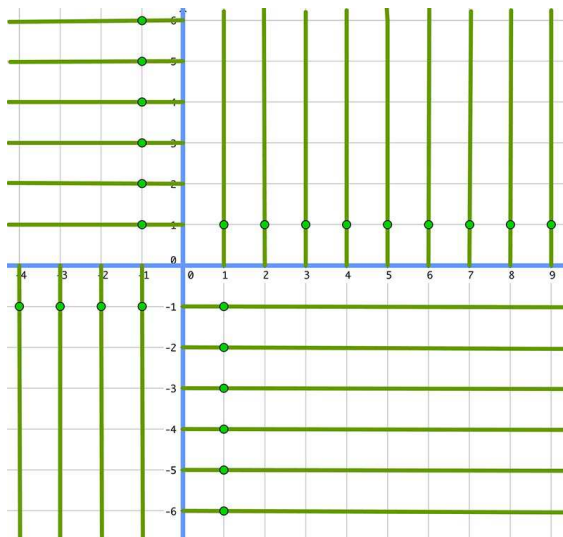

Figure 4: Trunks (blue) and branches (green) for the familiar square tiling, 4^4. Each vertex is associated (via a blue or green edge) with a unique vertex that is one step further away from P, except for the vertices on the (blue) trunk, where branches (green) have sprouted.
As four branches sprout at each distance $n > 0$ from P, joining the trunk to the four green vertices, the CS satisfies the recurrence $a(n+1) = a(n) + 4$.

Using the coloring book approach we draw "trunks" (in blue) and "branches" (in green) (see Fig. 4). Each vertex is associated (via a blue or green edge) with a unique vertex that is one step further away from P, except for the vertices on the (blue) trunk, where additional branches (green) have sprouted.[2] As four branches sprout at each distance n from P (the vertices marked with a green dot indicate the starts of the branches) the coordination sequence satisfies the recurrence $a(n+1) = a(n) + 4$. The recurrence starts with $a(0) = 1$, and so we have again shown that $a(n) = 1, 4, 8, 12, 16, 20, \ldots$, as in (1).

5 The Cairo tiling with respect to a tetravalent vertex

At left in Figure 2, the vertices in the Cairo tiling in the vicinity of a tetravalent vertex P are marked by contour lines of constant distance to P, and counting the vertices on each contour line confirms that the initial terms of the CS are as shown in (1).

The subgraph H is shown in Fig. 5 (left). There are four trunks (blue) and infinitely many branches (green), one branch originating at each trunk vertex. Figure 5 (right) shows one sector of H redrawn so that the trunks and branches are straight, and so that we can see they satisfy Property (ii) — that is, using edges that are not part of H (these edges are colored gray) does not provide any shorter paths to the base vertex.

---

[2]This example is slightly exceptional in that the trunks and branches are not orthogonal to the contour lines.

As each vertex on a trunk or branch is associated with another trunk or branch vertex further out, and four new branches are introduced at each distance $n > 0$ from the origin, $a(n+1) = a(n)+4$; noting that $a(1) = 4$, we have $a(n) = 4n$, $n > 0$, completing the proof of Theorem 1.

In the redrawn sector on the right of Fig. 5, all the points at a given distance from the base point are colinear, and we see that there are exactly $n - 1$ points in the interior of the sector at distance n from the base point. Taking into account the four branch points, we have another proof that $a(n) = 4(n - 1) + 4 = 4n$ for $n > 0$.

Note that there is a unique (green) branch originating at each (blue) trunk vertex. If the trunk vertex is at distance congruent to 1 or 2 mod 4 from the origin, the branch turns to the left, otherwise it turns to the right.
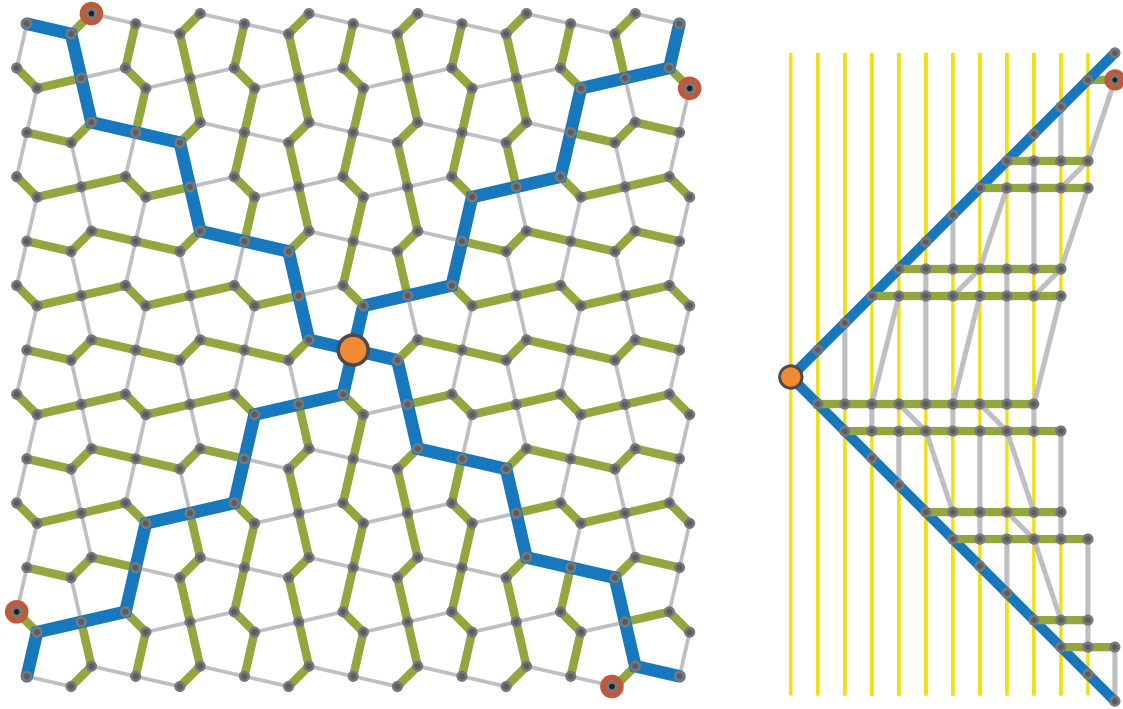

Figure 5: At left, the subgraph H for a tetravalent base vertex in the Cairo tiling. There are four congruent sectors. At right, the right-hand sector of H has been redrawn so that the blue trunks and green branches are straight, with horizontal distances equal to the distance back to P in G, in order to show that the (gray) edges not in H do not reduce the distance to the origin. Note that H is transverse to the contour lines, shown in yellow. At each distance $n + 1$ from P, all but four of the vertices (green) may be associated with the vertices at distance n, by tracing back one edge in H — hence $a(n + 1) = (n) + 4$. The four red dots on the periphery of the left figure indicate the division into sectors, and help match up the left and right figures.

6   The Cairo tiling with respect to a trivalent vertex

At right in Figure 2 we show the contour lines in the vicinity of a trivalent vertex P in the Cairo tiling, confirming that the initial terms of the CS are as shown in (2).

Because the graph now has only mirror symmetry, the subgraph H, is necessarily less elegant than in the tetravalent case. The best choice for H that we have found, shown in Fig. 6, now has six trunks, two of which sprout "twigs" shown in dark red.

As in Fig. 5, H is naturally divided into four sectors (ignoring the twigs for now). The right and top sectors are congruent to each other and the left and bottom sectors are essentially the same as any of the sectors in Fig. 5, the main difference being that the base vertices for these two sectors are now one edge away from the origin instead of being located at the origin.
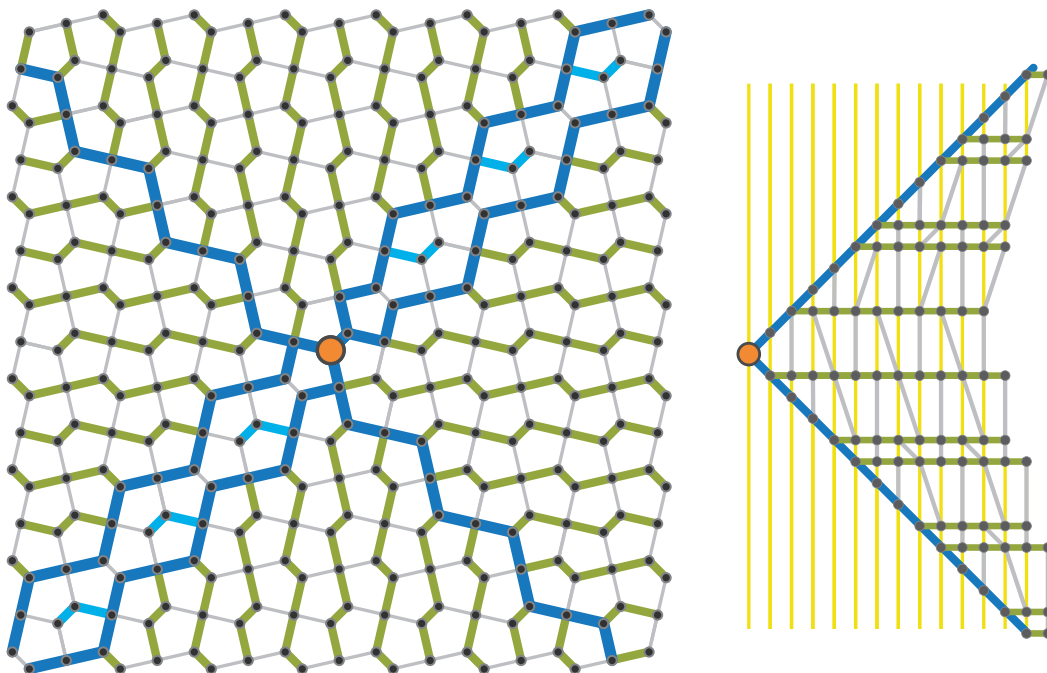

Figure 6:   At left, the subgraph H (the blue, green, and dark red edges) for the trivalent case. Two of our trunks have split down the middle, and moreover have sprouted "twigs" (light blue). In the right-hand illustration, the right sector has been redrawn so that the blue trunks and green branches are straight, in order to show that the (gray) edges not in H do not reduce the distances to the origin, and to make it easy to count the vertices at a given distance from the base point.

Although there is some variation from level to level, with two out of every three trunk nodes sprouting branches, and taking into account the periodic appearance of twigs, we obtain the recurrence

$$a(n+4) = a(n) + 16, \ n \geq 3$$

by observing that exactly 16 branches and twigs sprout in any four consecutive values of n, and consequently all but 16 vertices at distance $n + 4$ may be traced back and associated with the vertices at distance n, along a trunk, or branch, or from a twig to a closer twig. Verifying the terms

$a(0)$ through $a(6)$, we obtain $a(n)$ as in Theorem 2.

Again there is an alternative way to see this. In Fig. 6 (right), we see that the vertices at a given distance from the base point are colinear, and there are $n-2$ interior vertices in the right (and top) sectors if $n \equiv 0$ or 1 (mod 4), or $n-1$ if $n \equiv 2$ or 3 (mod 4). Putting this together with what we know from the previous section about the left and bottom sectors, and the easily counted trunk and twig vertices, we obtain equation (3).

7   The $3^2.4.3.4$ tiling

The $3^2.4.3.4$ tiling (Fig. 3 in §1) is a uniform tiling: all vertices are equivalent, and we can choose P to be any vertex. As in the previous section, the graph G has only mirror symmetry, and so again we have to accept that our subgraph H of trunks and branches will be less symmetrical that the graph in §5.

In our choice for H, shown in Fig. 7, there are two horizontal trunks, but on the vertical trunks some vertices on the vertical branches have been split into "burls" (creating loops of length 4). With the orientation shown, quadrants I and II are mirror images of each other, as are quadrants III and IV. One can see immediately that any simple path in H from a vertex back to P is as short as any other path back to P, and so Property (ii) is satisfied.
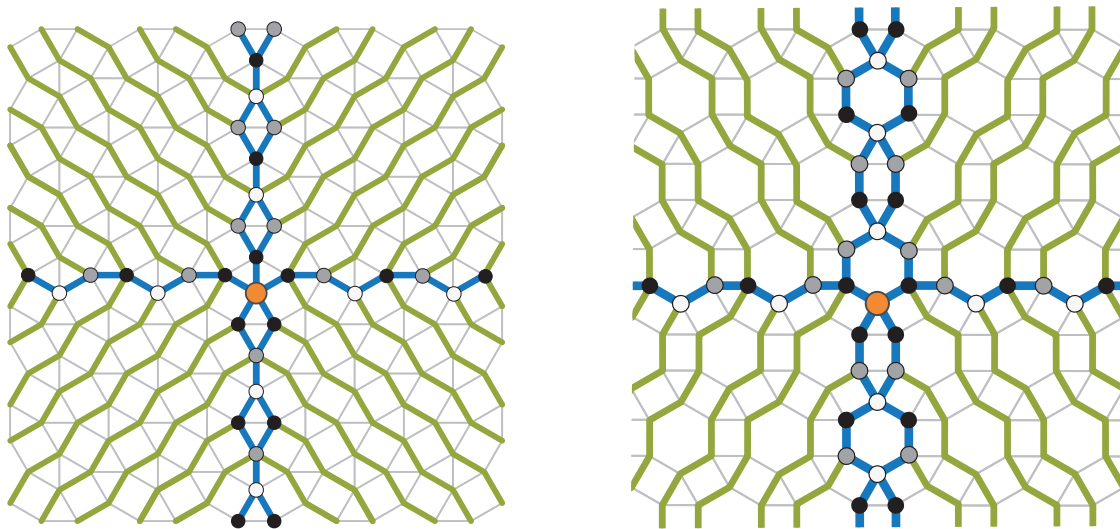

Figure 7:   Trunks and branches H for the $3^2.4.3.4$ tiling, at left and for the 3.4.6.4 tiling at right. In both drawings, the base vertex P is at the center and vertices on the blue trunks are colored by their distance to P mod 3 — 0 (white), 1 (black), or 2 (gray).

To calculate the coordination sequence, we may note that at any three consecutive distances $n+1, n+2, n+3, n > 0$ from P, 16 branches are introduced, and so all but 16 vertices at distance $n+3$ may be associated with those at distance n. This gives us the recurrence $a(n+3) = a(n)+16, n > 0$. Checking the terms $a(0) = 1, a(1) = 5, a(2) = 11, a(3) = 16$, we obtain (5), and so complete the proof of Theorem 3.

11

8 The $3.4.6.4$ tiling

Our next example is another uniform tiling, 3.4.6.4, and we will prove that this too has the same CS as the square grid (this establishes a 2014 conjecture of Darah Chavey stated in A008574).

Theorem 4. *The coordination sequence with respect to a vertex in the* 3.4.6.4 *tiling is given by* $a(0) = 1$, $a(n) = 4n$ *for* $n \geq 1$.

We show our choice of trunks and branches at the right in Fig. 7. As in the left-hand figure, the vertical trunks have split, producing burls which now are chains of hexagons. Again, quadrants I and II are mirror images of each other, as are quadrants III and IV. We can see that Property (ii) is satisfied and that the pattern propagates.

As a total of twelve branches are introduced at three consecutive levels $n+1$, $n+2$, $n+3$, $n > 1$, we have the recurrence $a(n+3) = a(n) + 12$. Checking the terms up to $a(4) = 16$, we complete the proof.

9 The bew tiling

The bew tiling (Fig. 8) is the first net in the current listing of two-dimensional nets in the [34] database, and is similar to the Cairo tiling in that there are two kinds of vertices , and the CS with respect to one of them is the same as the CS for the square grid. This tiling is easily analyzed by our method, and our discussion will be brief.

All the vertices are tetravalent. The first type of vertex is a 3.3.6.6 vertex, meaning that it is surrounded successively by a triangle, a triangle, a hexagon, and a hexagon. This is a vertex where two hexagons meet along an edge. We assume the tiling is oriented as in Fig˙ 8. The subgraph H is constructed to have mirror symmetry across the x-axis. There are four trunks, all simple paths, and the branches are also simple paths. The CS is easily seen to be the same as that in Theorem 1.

The second type of vertex is a 3.6.3.6 vertex, meaning that it is surrounded successively by a triangle, a hexagon, a triangle, and a hexagon. This is a vertex where two hexagons meet at a vertex. The CS begins

$$1, 4, 6, 14, 14, 22, 22, 30, 30, 38, 38, 46, 46, 54, 54, 62, 62, 70, 70, 78, \ldots, \tag{6}$$

(A296910). We leave the proof of the following to the reader, referring to Figure 8 (right).

Theorem 5. *The coordination sequence of the bew tiling with respect to a 3.6.3.6 vertex is given by* $a(0) = 1$, $a(1) = 4$, *and thereafter* $a(n) = 4n - 2(-1)^n$.
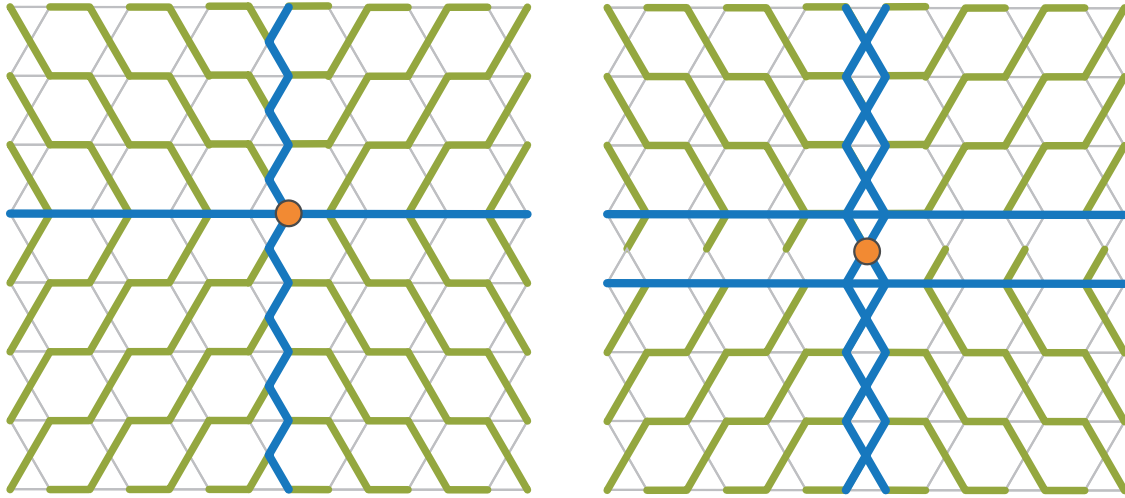
Figure 8: The 'bew' tiling, the first net listed in the RCSR database [34], has two kinds of vertex: a trivalent vertex, of the form 3.3.6.6, with mirror symmetry; and a tetravalent vertex, of the form 3.6.3.6, with rectangular symmetry (a Klein 4-group). The graph H for the first kind of vertex is on the left, and has mirror symmetry. The graph H for the second kind of vertex is on the right, and because of the twigs on the horizontal branches, has only 180° rotational symmetry.

10 The 4.8^2 tiling

Theorem 6. *The CS ([A008576](https://oeis.org/A008576)) with respect to a vertex in the 4.8^2 uniform tiling is given by $a(0) = 1$ and thereafter $a(3k) = 8k$, $a(3k + 1) = 8k + 3$, $a(3k + 2) = 8k + 5$.*

Proof. The subgraph H, shown in at left in Fig. 9 — we again resort to using "burls" but the proof is the same as before: H satisfies Property (ii) and may be propagated; for each $n > 1$, at three consecutive distances a total of 24 branches sprout. Consequently, for $n > 1$, $a(n+3) = a(n) + 24$. Verifying the terms through $a(4)$, we complete the proof. □

11 The 3.12^2 tiling

The 3.12^2 uniform tiling is shown at right in Fig. 9. The CS with respect to any vertex begins

$$1, 3, 4, 6, 8, 12, 14, 15, 18, 21, 22, 24, 28, 30, 30, 33, 38, 39, 38, 42, 48, \ldots . \tag{7}$$

This is sequence [A250122](https://oeis.org/A250122), where there is a conjectured formula from 2014 due to Joseph Myers which we can now prove is correct.

Theorem 7. *The coordination sequence for the 3.12^2 tiling is given by $a(0) = 1$, $a(1) = 3$, $a(2) = 4$, and thereafter $a(4k) = 10k - 2$, $a(4k + 1) = 9k + 3$, $a(4k + 2) = 8k + 6$, and $a(4k + 3) = 9k + 6$.*
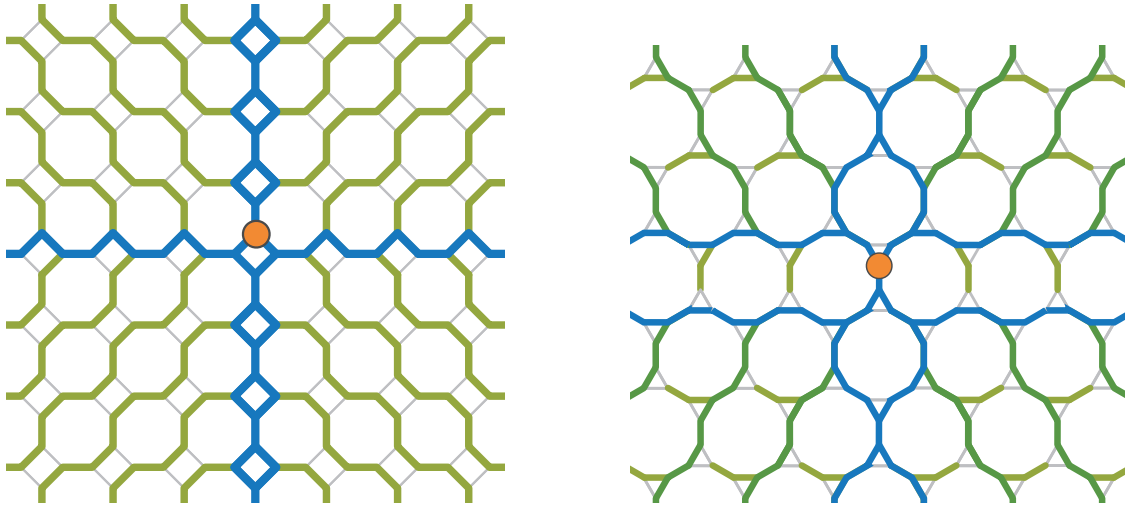
Figure 9: Trunks and branches H for the 4.8^2 tiling at left and the 3.12^2 tiling at right, with P at the center and trunks and branches H which clearly propagate and satisfy Property (ii).

The subgraph H is shown is shown at right in Fig. 9. The second quadrant is a mirror image of the first, and the third quadrant is a mirror image of the fourth. (The figure is not symmetric about the x-axis.) In the first quadrant there are infinitely many parallel branches (green) consisting of infinite paths, together with twigs (olive green) of length 2 originating at certain branch vertices.

When we compute the CS, we find that the number of vertices at distance n from the origin in the various regions depends on the value of $n \bmod 8$, and so what we actually prove is that for $n \geq 3$ we have

$$
\begin{aligned}
a(8k) &= 20k - 2, \\
a(8k+1) &= 18k + 3, \\
a(8k+2) &= 16k + 6, \\
a(8k+3) &= 18k + 6, \\
a(8k+4) &= 20k + 8, \\
a(8k+5) &= 18k + 12, \\
a(8k+6) &= 16k + 14, \\
a(8k+7) &= 18k + 15,
\end{aligned}
$$

which will imply the result in the theorem.

The count is more complicated for this example, firstly just because we have to match vertices at distance n from P to those at distance $n + 8$, but much more so because of the presence of the twigs. The direction taken by the twigs varies. Looking from the base vertex along a line to the North-East, the twigs on or to the left of this line turn to the left, and those to the right of the line turn to the right. A similar thing happens in the fourth quadrant.

In short, at different distances mod 8, there are different numbers of vertices on twigs, and varying numbers of vertices at distance $n + 8$ that are unmatched at distance n. Once this is taken

into account, it is straightforward to verify that the above equations hold, and the theorem follows.
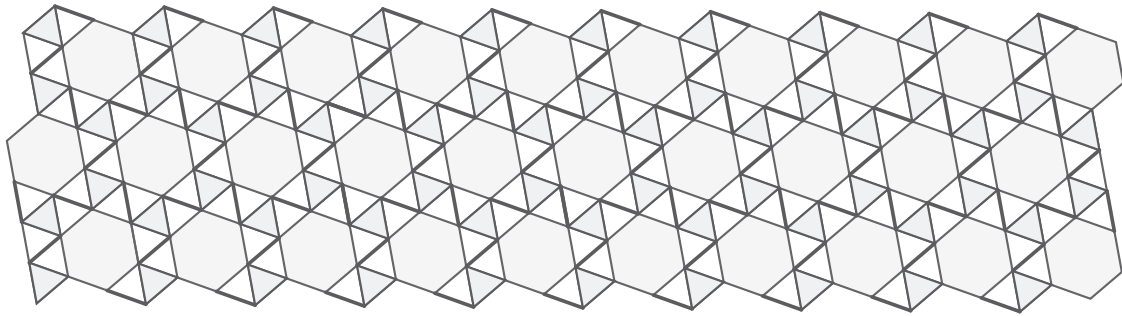

Figure 10: A portion of the $3^4.6$ uniform tiling.

12   The $3^4.6$ tiling

The $3^4.6$ uniform tiling is shown in Fig.10. This is also known as the snub $\{6,3\}$ tiling, and has symmetry group 632 in the orbifold notation. The CS with respect to any vertex begins

$$1, 5, 9, 15, 19, 24, 29, 33, 39, 43, 48, 53, 57, 63, 67, 72, 77, 81, 87, 91, \ldots . \tag{8}$$

This is sequence A250120, where there is a conjectured formula from 2014 due to several people, which we can now prove is correct.

Theorem 8. *The coordination sequence for the $3^4.6$ tiling is given by $a(0) = 1$, $a(1) = 5$, $a(2) = 9$, $a(3) = 15$, $a(4) = 19$, $a(5) = 24$ and for $n \geq 3$, $a(n + 5) = a(n) + 24$.*

The recurrence can also be written as $a(5k + r) = 24k + a(r)$ for $k \geq 0$, $0 \leq r \leq 4$.

In all our previous examples, we were able to use the coloring book method to find trunks and branches by simply drawing on a picture of the tiling. This enabled us to calculate the coordination sequence directly, bypassing any complexities in the contour lines. Compare, for example, the contour lines in Fig. 2 with the trunks and branches of Figures 5 and 6, which made the CS for the Cairo tiling a simple calculation. We were happy that this strategy has worked in every case up to this point.

Of course, to use the coloring book method, we must also confirm, in some inductive manner, that the trunks and branches can be continued indefinitely and satisfy Property (ii). For the Cairo tiling, we redrew two of the sectors so as to make it clear that there were patterns of local structure that propagated outwards, maintaining a valid trunks and branches structure that made it easy to compute the CS. We were not as explicit in the next few examples, leaving to the reader the easy verification that the trunks and branches structure propagated. In the present section and the next, however, the structures are more complicated and so we must be more cautious.

We could have always used the contour lines directly, at least in principle — defining the contour lines recursively, with production rules that are constrained by local conditions, as in [21].

For tilings with a co-compact symmetry, such as the ones in this paper, contour lines can be used to conjecture, calculate, and give proofs for the recurrences satisfied by the coordination sequences.

The contour lines for the $3^4.6$ tiling are shown in Fig. 11. From this we can verify that, at least initially, the number of vertices at distance $n > 1$ from the base vertex increases by exactly 24 when n is increased by 5. Although there appear to be a lot of individual cases to consider, the contours are highly ordered, and the task is primarily one of cataloging the local structures.
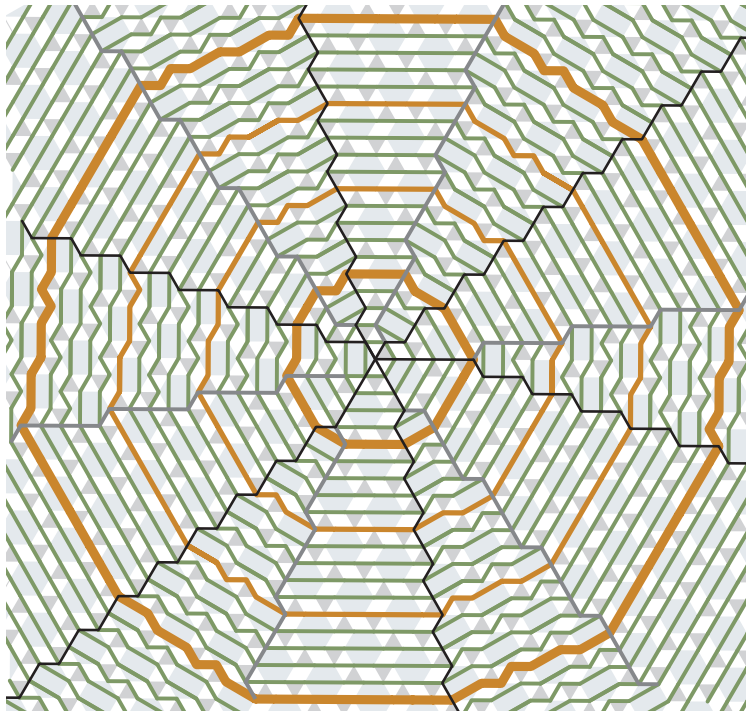

Figure 11: The contour lines of the $3^4.6$ tiling; their lengths form sequence A250120. The contour lines are partitioned into twelve sectors, alternatively straight and zig-zag. The boundaries zig-zag-to-straight (reading clockwise), drawn in black, have period 3. The boundaries straight-to-zig-zag, drawn in gray, have period 5 — in each sector the patterns at the ends of a contour segment have period 15. A pair of contours 15 steps apart are emphasized in the figure by heavy brown lines. With patience, after another 15 steps the regular structure becomes more apparent. Even without doing that, with care one can verify that from each level $n > 1$ to level $n + 5$, the number of vertices increases by 24. In Fig. 12, we use a trunks and branches structure to make this more transparent.

Outside of an initial region about P, there are really only four kinds of vertex neighborhoods to consider: vertices where the contour lines are straight, where they zig-zag, and where there is a transition from zig-zag-to-straight and *vice versa*. In each case, the underlying structure is straightforward and it is easy to see that it propagates from level to level, and also that the structure we see at the center — twelve sectors of alternating types, the six sectors of each type being fundamentally the same — must continue across the entire infinite tiling.

However, there is a further complexity: the boundaries between straight-to-zig-zag, drawn in black in Fig. 11, have a period-3 pattern, and so the structure of the segments crossing each sector recurs with period 15.

We now use a trunks and branches approach to simplify this structure, verifying locally that this give the CS, but without needing to check that there is a detailed match with the contour lines.
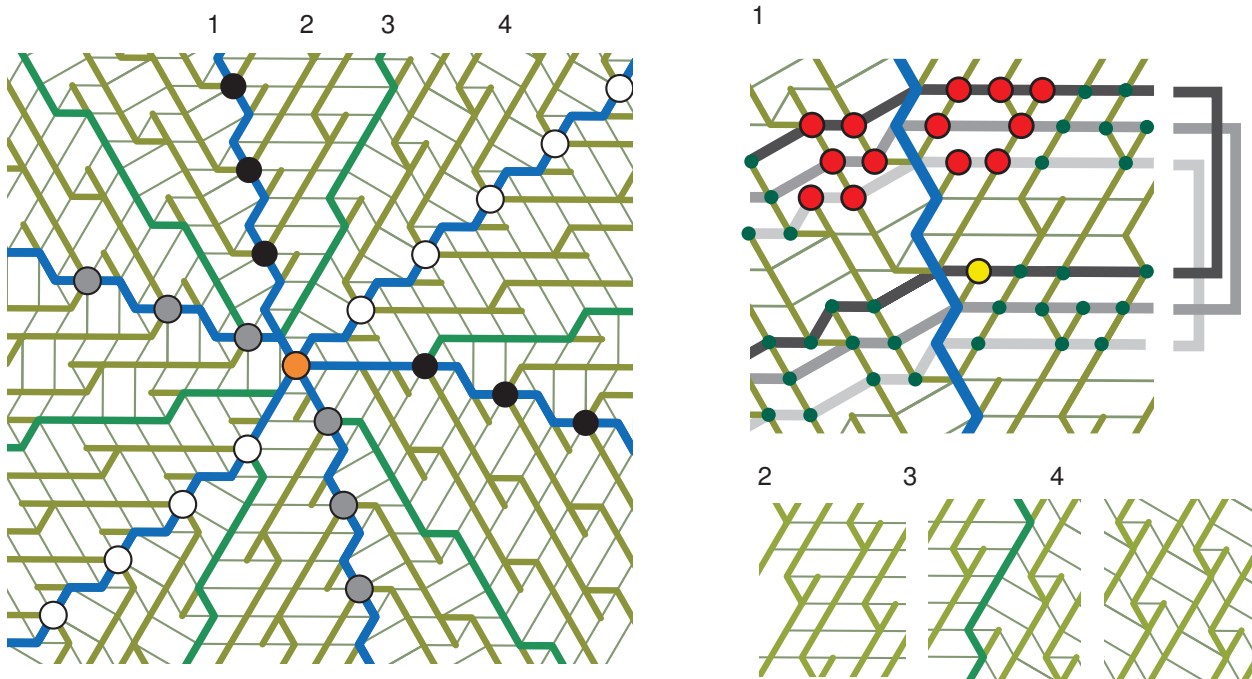

Figure 12: A trunks and branches structure for the $3^4.6$ tiling (left). Four patterns (1)-(4) that self-perpetuate from level to level (right).

The trunks and branches structure is shown on the left in Fig. 12. As in Fig. 7, the base vertex P is at the center and vertices on the blue trunks are colored by their distance to P mod 3 — 0 (white), 1 (black), or 2 (gray). The six trunks each produce a pair of branches and a twig at every third level, but shifted in pairs: all together the trunks sprout four branches and four twigs at each level. On the right in Fig. 12 are shown four patterns (1)-(4) that are self-perpetuating from level to level. If the boundary of a disk can be described by this atlas of patterns, then it is inside a larger disk with the same property — though one must carefully check that every transition from zig-zag-to-straight is of this precise form. By induction, the alleged contour lines in the pattern are nested simple closed curves and so can only lie on actual contour lines; thus the trunks and branches satisfy Property (ii) and correctly give the CS. With the exception of the red and yellow vertices in pattern (1), each vertex at level $n + 5$ is naturally matched with a vertex at level n, just by following a branch backwards. Notice that the branches have matching twigs at every fifth level. In pattern (1), we examine the mismatched vertices: the red vertices have no match five levels earlier, and the yellow vertex has no match five levels forward. Since pattern (1) repeats at every third level, we have considered all possible cases. At each level, two of the trunks show each of the three cases in pattern (1), so the number of vertices satisfies $a(n+5) = 24 + a(n)$ for $n \geq 3$, a net increase of six vertices per trunk. After explicitly verifying the initial terms of the coordination sequence, we have completed the proof of Theorem 8.
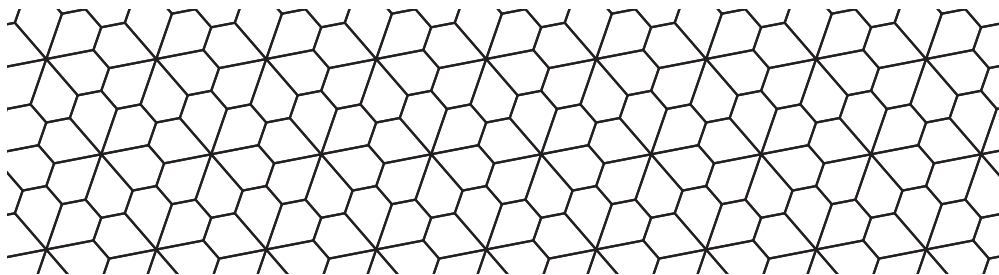
17

13   The snub-632 tiling

Figure 13: The snub-632 tiling.

We began this article by analyzing the Cairo tiling, which is the dual to the $3^2.4.3.4$ uniform tiling. Our final example is the snub-632 tiling (Fig. 13), which is the dual to the $3^4.6$ uniform tiling of the previous section. Like the Cairo tiling, this is a beautiful tiling; fundamentally it is the dual of the snub versions of both the 6^3 and 3^6 tilings. It has several names including:

- , a quotient of its edges as a graph on an orbifold [8, Ch.15],

- the 6-fold pentille tiling [8, pp. 288],

- the fsz-d net [34],

- and the dual of the $3^4.6$ tiling [25, pp. 63, 96, 480 (Fig. P_5-16)], which itself is the snub of the

  $\{3, 6\}$ tiling, with doily symbol $[0](12)(34) \cdot (3, 6, 3, 3, 3)$, encoding a collared graph on an orbifold.

We will refer to it simply as the snub-632 tiling. There is only one shape of tile, an elongated pentagon. (Again, as long as the underlying topology of the graph is preserved, small variations in the ratios of the sides do not affect the coordination sequences.) There are three types of vertices: (a) hexavalent vertices, with six-fold rotational symmetry, where six long edges of the pentagons meet; (b) trivalent vertices, with three-fold rotational symmetry, where three short edges meet; and (c) trivalent vertices, with no symmetry, where two short edges and one long edge meet. The coordination sequences (A298016, A298015, A298014) for these three types of vertices begin

$$(a) \quad 1, 6, 12, 12, 24, 36, 24, 42, 60, 36, 60, 84, 48, 78, 108, 60, 96, 132, 72, \ldots ,$$
$$(b) \quad 1, 3, 6, 15, 24, 18, 33, 48, 30, 51, 72, 42, 69, 96, 54, 87, 120, 66, 105, \ldots ,$$
$$(c) \quad 1, 3, 9, 15, 18, 27, 37, 37, 44, 57, 54, 61, 77, 71, 78, 97, 88, 95, 117, 105, \ldots \qquad (9)$$

Theorem 9. *The CS for the three types of vertices in the snub-632 tiling are given by:*
(a) $a(3k) = 12k$, $a(3k + 1) = 18k + 6$, $a(3k + 2) = 24k + 12$ for $k \geq 1$,
(b) $a(3k) = 18k - 3$, $a(3k + 1) = 24k$, $a(3k + 2) = 12k + 6$ for $k \geq 2$,
(c) $a(3k) = 20k - 3$, $a(3k + 1) = 17k + 3$, $a(3k + 2) = 17k + 10$ for $k \geq 2$,
with initial values as in (9). In each case we have $a(n) = 2a(n - 3) - a(n - 6)$ for $n \geq 8$.

18

We could prove Theorem 9 by working directly with the contour lines, which are shown in Figure 14, and demonstrating that a natural — if unwieldy — recursive structure holds for each of the three types of vertices. However, the coloring book approach will enable us to give a uniform treatment.
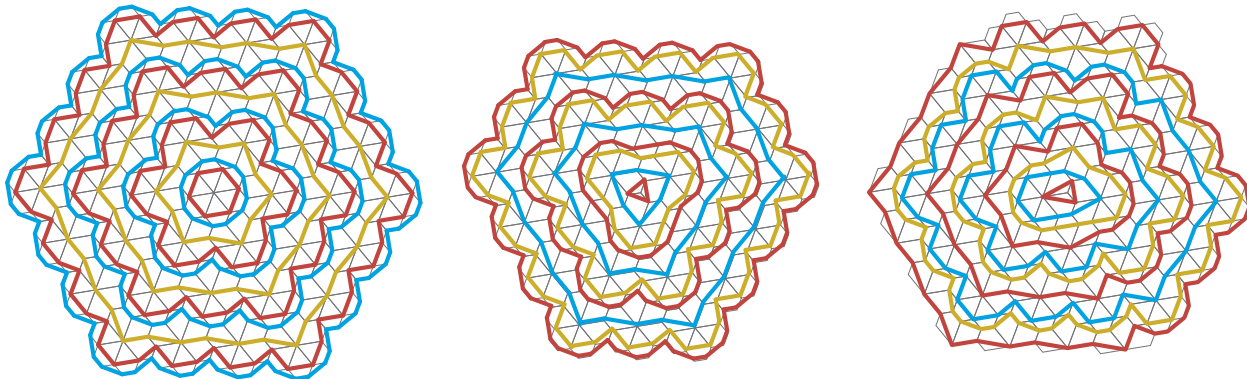

Figure 14: Contour lines in the snub-632, centered on a six-fold, three-fold and asymmetric vertex; they are clearly structured and we could compute with them directly. But the coloring book approach simplifies and unifies the count.

Figure 15 shows the trunks and branches structures for the three types of vertices, which we will continue to refer to as cases (a), (b), and (c) for a 6-fold, 3-fold, and asymmetric base vertex, respectively. Each figure is divided into 60-degree sectors, some of which are separated by channels. The individual sectors are all the same, although they differ in how far the apex of the sector (yellow) is from the base vertex (red). In case (a) all six sectors have apex at the base vertex, in case (b) the base vertex is two steps away from the apex, in two different ways, and in case (c) the base vertex is one, two or three steps away from the apex, in six different ways (now each sector has a different displacement from the base vertex).

Figure 16 shows a sector (internally they are all the same) with a channel next to it. The sector is bounded by two trunks (blue) and has a pattern of branches (red) and twigs (green). The figure also shows the contour lines defined by the distances to the apex (yellow). Contours at distances congruent to 0, 1, and 2 mod 3 from the apex are colored light gray, dark gray, and black, respectively. One can easily check that these contour lines are still the contour lines with respect to the base vertex, even when the base vertex is at one of the other eight possible vertices — there are no shortcuts to the base vertex. Of course the distances from the contours to the base vertex get increased by one, two, or three steps when the base vertex is moved. We return to this point in Fig. 17.

In the sector, the vertices at distance $n + 3$ from the apex are in one-to-one correspondence with the vertices at distance n, with the exception of the nine vertices shown in red on the right of Fig. 16. There are two unmatched vertices at distance 0 mod 3 from the apex (on the light gray curve), three at distance 1 mod 3 (on the dark gray curve) and four at distance 2 mod 3 (on the black curve). As the structure along a trunk repeats with period 3, this includes all the possibilities. The vertices that are not in any sector are in exact correspondence with those three steps further away.
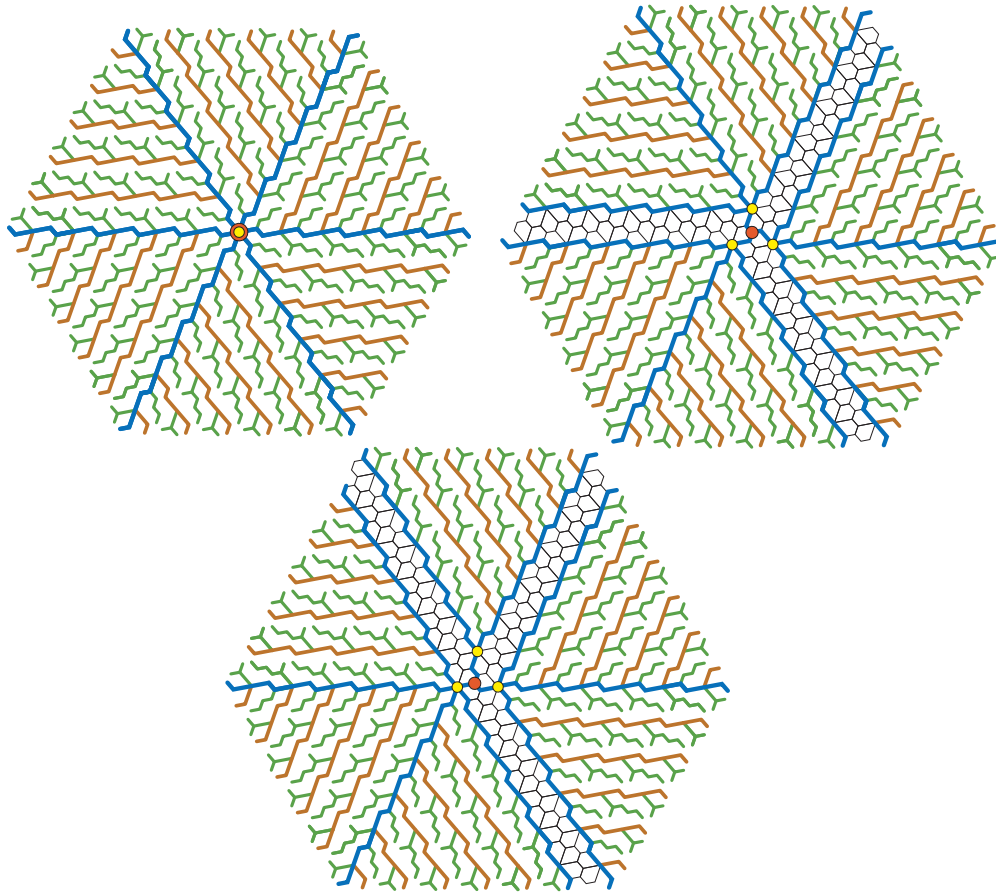
Figure 15: Trunks and branches structures for the three types of base vertices in the the snub-632 tiling: (a) (top left), 6-fold base vertex, (b) (top right), 3-fold, (c) (bottom) asymmetric. Each figure is divided into 60-degree sectors, some of which are separated by channels. The base vertex P is shown in red and the vertices at the apices of the sectors in yellow.

The detailed book-keeping for case (c) is as follows.

In case (c), take n sufficiently large, which turns out to mean $n > 5$, which is the distance from P to where the regular structure starts to be self-perpetuating. There is one sector with apex at distance 3; so from P, there are, for

$\quad n = 0 \mod 3, \quad$ two unmatched vertices at $n + 3$,
$\quad n = 1 \mod 3, \quad$ three unmatched at $n + 3$,
$\quad n = 2 \mod 3, \quad$ four unmatched at $n + 3$.

There are two sectors with apex at distance 2, so from P there are

n=2 mod 3, twice two unmatched vertices at $n + 3$,
n=0 mod 3, twice three unmatched at $n + 3$,
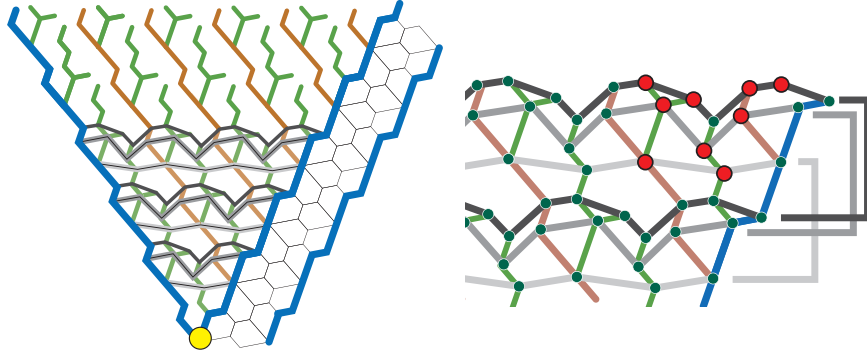n=1 mod 3, twice four unmatched at $n + 3$.

Figure 16: On the left, a sector and a channel, showing trunks (blue), branches (red), twigs (green), and contours (light grey, dark gray, and black) defined by distances to the apex (yellow). In the sector, the vertices at distance $n + 3$ from the apex are in one-to-one correspondence with the vertices at distance n, with the exception of those shown in red at right.

There are three sectors with apex at distance 1, so from P there are

$n = 1 \mod 3$, three times two unmatched vertices at $n + 3$,
$n = 2 \mod 3$, three times three unmatched at $n + 3$,
$n = 0 \mod 3$, three times four unmatched at $n + 3$

In summary, for case (c) there are three sectors with apex at distance 1 from P, two at distance 2 and one at distance 3. The vertices in the channels do not contribute to the recursion (since the vertices at distance $n + 3$ are in one-to-one correspondence with those at distance n, for $n > 2$). For case (c) we therefore have the recurrence, for $k > 1$,

$$a(3k + 6) = 3 \cdot 4 + 2 \cdot 3 + 1 \cdot 2 + a(3k + 3),$$
$$a(3k + 7) = 3 \cdot 2 + 2 \cdot 4 + 1 \cdot 3 + a(3k + 4),$$
$$a(3k + 8) = 3 \cdot 3 + 2 \cdot 2 + 1 \cdot 4 + a(3k + 5).$$

Cases (a) and (b) are similar (but simpler):

In case (a), there are six sectors, each with apex at distance 0 from P. The recurrence is therefore, for $k > 1$, $a(3k+3) = 6 \cdot 2 + a(3k+0)$, $a(3k+4) = 6 \cdot 3 + a(3k+1)$, $a(3k+5) = 6 \cdot 4 + a(3k+2)$.

For case (b), there are six sectors, each with apex at distance 2 from P, and the recurrence is, for $k > 1$, $a(3k + 5) = 6 \cdot 2 + a(3k + 2)$, $a(3k + 6) = 6 \cdot 3 + a(3k + 3)$, $a(3k + 7) = 6 \cdot 4 + a(3k + 4)$.

After verifying the initial terms by hand, we recover the sequences stated in the theorem.

However, as mentioned above, we must still check that even when the base vertex P is not at the apex, the contour lines measured from P really do cross the sectors and their trunks and branches structures as shown in Figure 16. This check is carried out in Figure 17. The heavy lines indicate where the regular structure — the recurrence — begins.
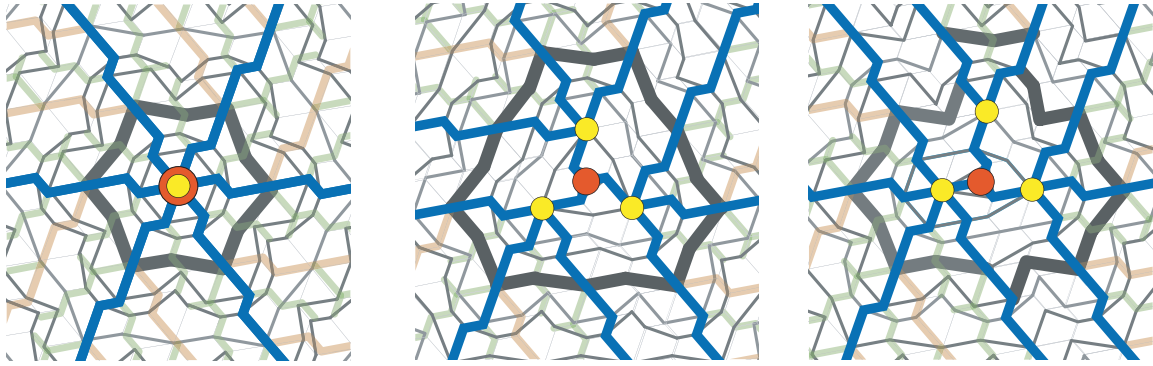
Figure 17: The contour lines near P in each of the cases (a), (b) and (c).

14 Cayley diagrams and growth series

If the symmetry group of the tiling acts transitively on the vertices, as it does for uniform tilings, in principle[3] it is possible to represent the graph of the tiling as a Cayley diagram for an appropriate presentation of the group. For example, consider the 4.8^2 tiling shown in Fig. 9. Every vertex is trivalent, with one edge at the vertex (denoted "o", say) separating two adjacent octagons, and a pair of edges ("ℓ" and "r") that go either to the left or the right around the adjacent square. Let R mean 'move along the edge o', and let S mean 'move along the edge ℓ'. Applying R twice returns one to the start, which we indicate by saying that $R^2 = 1$. Similarly, $S^4 = 1$ (going around the square) and $(RS)^4 = 1$ (going around an octagon). The group G generated by R and S subject to these relations, specified by the presentation

$$G = \langle R, S \mid R^2 = S^4 = (RS)^4 = 1 \rangle, \tag{10}$$

assigns a unique label to each vertex in the graph. In technical terms, this gives an identification of the graph of the tiling with the Cayley diagram of the group defined by this presentation [27].

The 'length' of a group element is the minimal number oi generators needed to represent it, which is also its distance from the identity element in the Cayley diagram. The 'growth function' for the group specifies the number of elements of each length n, and so the growth function is precisely the coordination sequence for the tiling. For the graphs of uniform tilings, the Knuth-Bendix algorithm [28, 19] can be used to solve the word problem[4] and determine the growth function. This algorithm is implemented in the GrowthFunction command in the computer algebra system Magma [6]. When applied to the presentation (10), for example, Magma returns the generating function

$$\sum_{n=0}^{\infty} a(n)x^n = \frac{(1+x)^2}{(1-x)^2},$$

which is equivalent to the formulas given in Theorem 6.

Table 1 lists presentations for all eleven uniform two-dimensional tilings. We have verified that the resulting growth functions coincide with the coordination sequences given in earlier sections and in [32].

---

[3]In practice, this is straightforward in two dimensions, but not at all easy in three dimensions.
[4]Although in general this problem is insoluble.

Table 1: Presentations for the groups of the eleven uniform tilings, giving section number if mentioned above, number of generators g, and corresponding sequence number.

Tiling	§	g	Presentation	Sequence
3^6		3	$RST = 1, RS = SR$	A008458
$3^4.6$	12	3	$R^2 = S^3 = T^6 = RST = 1$	A250120
$3^3.4^2$		4	$R^2 = T^2 = U^2 = SUT = 1, RS = SR$	A008706
$3^2.4.3.4$	7	3	$R^2 = RST = (ST^{-1})^2 = 1$	A219529
$3.4.6.4$	8	2	$R^3 = S^6 = RSRS = 1$	A008574
$3.6.3.6$		2	$R^3 = S^3 = (RS)^3 = 1$	A008579
3.12^2	11	2	$R^2 = S^3 = (RS)^6 = 1$	A250122
4^4	3	2	$RS = SR$	A008574
$4.6.12$		3	$R^2 = S^2 = T^2 = (TS)^2 = (RT)^3 = (SR)^6 = 1$	A072154
4.8^2	10	2	$R^2 = S^4 = (RS)^4 = 1$	A008576
6^3		3	$R^2 = S^2 = T^2 = 1, RST = TSR$	A008486

Presentations for the 17 planar crystallographic groups can be found in [10, Table 3], and in 2003 Shutov [35] used them to compute coordination sequences for the corresponding *directed* Cayley graphs. Eon [18] gives presentations for the eleven uniform tilings and points out the connection between the Cayley diagrams and the graphs of the tilings. However, neither article uses these presentations to explicitly compute the coordination sequences for the tilings.

It is worth pointing out that the growth series approach to finding coordination sequences used in this section only applies when the graph of the tiling coincides with the Cayley graph of some group, whereas our coloring book approach can potentially be applied to any periodic tiling.

Acknowledgment

After seeing a preliminary version of this article, Professor Jean-Guillaume Eon commented that the coloring book method might be viewed as complementary to the algebraic method introduced in [13]. The labeled quotient graph of the net or tiling from that article could help to find the subgraph H needed for our approach, and conversely, using H instead of the quotient graph may simplify finding the the coordination sequence.

It will be interesting to see if a combination of our methods will lead to proofs of the conjectured formulas for some of the more complicated tilings, such as those of the 20 2-uniform tilings. A list of these 2-uniform tilings and their coordination sequences (and conjectured formulas) may be found in entry A301724 in [32].

References

[1] M. Baake and U. Grimm, Coordination sequences for root lattices and related graphs, *Zeit. f. Krist.*, **212** (1997), 253–256.

[2] R. Bacher and P. de la Harpe., Conjugacy growth series of some infinitely generated groups, *Internat. Math. Res. Notices*, **2018:5** (2018), 1532–1584; https://hal.archives-ouvertes.fr/hal-01285685/document.

[3] R. Bacher, P. de la Harpe, and B. Venkov, Séries de croissance et series d'Ehrhart associées aux réseaux de racines, *C. R. Acad. Sci. Paris, Sér. 1*, **325** (1997), 1137–1142.

[4] D. Bailey, Cairo Tiling, in http://www.tess-elation.co.uk/cairo-tiling.

[5] V. A. Blatov, A. P. Shevchenko, and D. M. Proserpio, Applied topological analysis of crystal structures with the program package ToposPro, *Cryst. Growth Des.*, **14** (2014), 3576-3586; http://topospro.com.

[6] W. Bosma, J. Cannon, and C. Playoust, The Magma algebra system. I, The user language, *J. Symbolic Comput.*, **24** (1997), 235-265.

[7] D. Chavey, Tilings by regular polygons II: A catalog of tilings, *Computers & Mathematics with Applications*, **17:1–3** (1989), 147–165.

[8] J. H. Conway, H. Burgheil, and C. Goodman-Strauss, *The Symmetries of Things*, A. K. Peters, Wellesley, MA, 2008.

[9] J. H. Conway and N. J. A. Sloane, Low-Dimensional Lattices VII: Coordination Sequences, *Proc. Royal Soc. London, Series A*, **453** (1997), 2369–2389.

[10] H. S. M. Coxeter and W. O. J. Moser, *Generators and Relations for Discrete Groups*, Springer, 4th. ed., 1984.

[11] P. de la Harpe, *Topics in Geometric Group Theory*, Univ. Chicago Press, 2000,

[12] O. Delgado-Friedrichs and M. O'Keeffe, Edge-transitive lattice nets, *Acta Cryst.*, **A65** (2009), 360-363.

[13] J.-G. Eon, Algebraic determination of generating functions for coordination sequences in crystal structures, *Acta Cryst.*, **A58** (2002), 47–53.

[14] J.-G. Eon, Topological density of nets: a direct calculation, *Acta Cryst.*, **A60** (2004), 7–18.

[15] J.-G. Eon, Infinite geodesic paths and fibers, new topological invariants in periodic graphs, *Acta Cryst.*, **A63** (2007), 53–65.

[16] J.-G. Eon, Topological density of lattice nets, *Acta Cryst.*, **A69** (2013), 3 pages.

[17] J.-G. Eon, Topological features in crystal structures: a quotient graph assisted analysis of underlying nets and their embeddings, *Acta Cryst.*, **A72** (2016), 268–293.

[18] J.-G. Eon, Symmetry and topology: the 11 uninodal planar nets revisited, *Symmetry*, **10** (2018), 13 pages; http://www.mdpi.com/2073-8994/10/2/35/htm.

[19] D. B. A. Epstein, D. F. Holt, and S. E. Rees, The use of Knuth-Bendix methods to solve the wordproblem in automatic groups, *J. Symbolic Computation*, **12** (1991), 397–414.

[20] B. Galebach, *N-uniform Tilings*, http://probabilitysports.com/tilings.html.

[21] C. Goodman-Strauss, Regular production systems and triangle tilings, *Theoret. Comp. Sci.*, **410** (2009), 1534–1549.

[22] C. Goodman-Strauss and N. J. A. Sloane, *A Tiling Coloring Book*, 2018 (in preparation).

[23] R. W. Grosse-Kunstleve, G. O. Brunner, and N. J. A. Sloane, Algebraic description of coordination sequences and exact topological densities for zeolites, *Acta Cryst.*, **A52** (1996), 879–889.

[24] B. Grünbaum and G. C. Shephard, Tilings by regular polygons, *Math. Magazine*, **50** (1977), 227–247.

[25] B. Grünbaum and G. C. Shephard, *Tilings and Patterns*, W. H. Freeman, New York, 1987.

[26] M. Hartley, *Archimedean Tiling Graph Paper*, http://www.dr-mikes-math-games-for-kids.com/archimedean-graph-paper.html.

[27] D. L. Johnson, *Presentations of Groups*, Cambridge Univ. Press, 1976.

[28] D. E. Knuth and P. B. Bendix. Simple word problems in universal algebras, in J. Leech, ed., *Computational Problems in Abstract Algebra*, Pergamon Press, Oxford, pp. 263–297. 1970.

[29] M. O'Keeffe, Coordination sequences for lattices, *Zeit. f. Krist.*, **210** (1995), 905-908.

[30] M. O'Keeffe and B. G. Hyde, Plane nets in crystal chemistry, *Phil. Trans. Royal Soc. London*, Series A, Mathematical and Physical Sciences, **295:1417** (1980), 553-618.

[31] M. O'Keeffe, M. A. Peskov, S. J. Ramsden, and O. M. Yaghi, The reticular chemistry structure resource (RCSR) database of, and symbols for, crystal nets, *Accounts of Chemical Research*, **41.12** (2008), 1782–1789.

[32] The OEIS Foundation Inc., *The On-Line Encyclopedia of Integer Sequences*, https://oeis.org.

[33] Printable Paper, *Graph Paper*, https://www.printablepaper.net/category/graph.

[34] Reticular Chemistry Structure Resource (RCSR), http://rcsr.net.

[35] A. V. Shutov, On the number of words of a given length in plane crystallographic groups (Russian), *Zap. Nauchn. Sem. S.-Peterburg. Otdel. Mat. Inst. Steklov. (POMI)*, **302** (2003), *Anal. Teor. Chisel i Teor. Funkts.*, **19**, 188–197, 203; English translation in *J. Math. Sci. (N.Y.)*, **129** (2005:3), 3922–3926 [MR2023041].

[36] L. van den Broek, §6: Investigation, http://www.ratio.ru.nl/lesmateriaal/angles/6_onderzoek.html.

[37] Wikipedia, *Cairo Pentagonal Tiling*, https://en.wikipedia.org/wiki/Cairo_pentagonal_tiling.

[38] Wikipedia, *List of Convex Uniform Tilings*, https://en.wikipedia.org/wiki/List_of_convex_uniform_